Current Optics and Photonics
Vol. 2, No. 1, February 2018, pp. 96-100

ISSN: 2508-7266(Print) / ISSN: 2508-7274(Online)
DOI: https://doi.org/10.3807/COPP.2018.2.1.096

Tunable Low Phase-noise Microwave Generation Utilizing an Optoelectronic Oscillator and a Fiber Bragg Grating

Zhuansun Xiaobo[1], Chen Yiwang[1], Zhang Pin[1]*, Yin Qin[1], Ni Jiazheng[2], and Dong Xiaohua[1]

[1]*Army Engineering University, Nanjing, Jiangsu 210014, China*
[2]*PLA Navy Research Institute, Beijing 100161, China*

(Received November 30, 2017 : revised January 15, 2018 : accepted January 16, 2018)

A tunable low-phase-noise microwave generation structure that utilizes an optoelectronic oscillator (OEO) and a fiber Bragg grating (FBG) is proposed and experimentally demonstrated in this article. This structure has no particular requirement for the band width of the laser, and its tunability is realized through adjusting the central frequency of the tunable FBG. A detailed theoretical analysis is established and confirmed via an experiment. A high-purity microwave signal with a frequency tunable from 6 to 12 GHz is generated. The single-sideband phase noise of the generated signal at 10.2 GHz is -117.2 dBc/Hz, at a frequency offset of 10 kHz.

Keywords : Low phase-noise, Microwave generation, Optoelectronic oscillator, Tunable FBG
OCIS codes : (240.6380) Spectroscopy, modulation; (250.4110) Modulators

I. INTRODUCTION

The optoelectronic oscillator was first investigated by Maleki and Yao in 1996 [1, 2], and in recent years, has been considered as an effective and popular means of generating high-frequency and ultra low-phase noise microwave signals. It is applied to perform navigation, communications, radar, and measurements. The traditional optoelectronic oscillator (OEO) consist of some microwave devices and some optical devices, such as laser, optical fiber, photoelectric detector (PD), amplifier (AMP) and modulator.

The major limitations of a conventional OEO is limited frequency tenability, because an electrical bandpass filter (BPF), which usually has a low, fixed central frequency, is employed for single-frequency operation [3]. Many solutions to this problem have been proposed to improve the frequency-tunable range by frequency multiplying [4] or using a tunable microwave photonic filter [5-7]. For example, Xiaopeng Xie from Peking University designed an OEO structure using a phase modulator (PM) and a narrow band tunable optical bandpass filter (TOBF) [8]. Wei Chen from Xidian University proposed a structure using a dual parallel Mach Zehnder modulator (DPMZM) and a fiber Bragg grating to generate a quadruple frequency signal at about 24 GHz [9]. Bo Yang proposed an X-band signal generator with frequency tunable from 8.4 to 11.8 GHz [10]. Recently several viable OEO structures have been proposed, such as an OEO consisting of a phase-shifted fiber Bragg grating (PS-FBG) [11, 12] or apodized fiber Bragg grating (A-FBG) [13, 14] and a phase modulation, with a large tunable frequency range (over 10 GHz). However, the frequency of the radio-frequency (rf) signal from the OEO is sensitive to the quality of the laser source. Therefore, this structure is difficult to realize and expensive.

In this paper a small, inexpensive OEO structure is proposed, which can generate a signal that is tunable over a wide frequency range. We demonstrate the feasibility of a tunable OEO using a tunable FBG both theoretically and experimentally and then study the dynamic laws of this OEO. Experimentally, a wide frequency range from 6 to 12 GHz and a 60 dB suppression ratio are realized. The phase noise of the generated signal was measured, revealing that the single-sideband phase noise of a 10.2 GHz signal was -117.2 dBc/Hz at an offset of 10 kHz.

*Corresponding author: pinzhangfour@126.com, ORCID 0000-0002-2806-5768
Color versions of one or more of the figures in this paper are available online.

II. PRINCIPLE

The experimental setup for the tunable OEO is established in this section. Figure 1 shows a schematic of the proposed tunable OEO. The frequency-tunable oscillator is mainly composed of a distributed feedback laser (DFB), a Mach Zehnder modulator (MZM), a PD, a single mode fiber (SMF), an amplifier and a tunable FBG. Light from the DFB is sent to the MZM, which modulates the feedback signal into light. The modulated light spreads through the optical fiber, which is used to obtain a high Q value. The light is then transmitted to a tunable FBG, whose reflected light frequency can be varied by turning the grating. The tunable FBG is embedded in the OEO loop by an optical circulator. An electronic spectrum analyzer measures the output rf signal.

When a difference in frequency exists between the reflected light and the laser, the PD generates an rf signal via the beat frequency. The beat signal is electrically amplified and fed back to the MZM to realize the OEO. The frequency of the output rf signal is determined by the FBG's reflected light; thus the tuning range of the output signal is influenced by the effective range of the tunable FBG and other optoelectronic devices.

An FBG is a type of optical fiber that has a periodic perturbation of refractive index along the fiber's length. It is formed by exposure of the core to an intense optical-interference pattern. It can reflect the incident light at a central wavelength, and this process follows Braggs law. The central wavelength of the reflection is given by

$$\lambda_{Bragg} = 2n_{eff}\Lambda \tag{1}$$

where n_{eff} is the modal index and Λ is the grating's period. The tunable FBG we used is a variable-grating-period FBG [15].

The single loop transfer process is shown in Fig. 2.

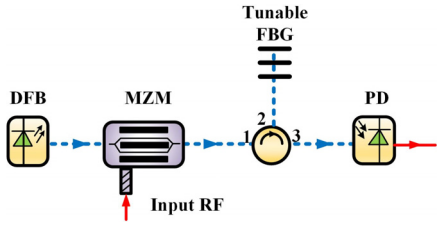

FIG. 2. The single-loop transfer process of the OEO.

The output electric field from the laser can be expressed as

$$E_1(t) = \int_{-\infty}^{+\infty} F(w)e^{jwt}dw \tag{2}$$

Assume that $F(w)$ follows a Gaussian distribution; then, $F(w) = Ae^{-\frac{(w-w_c)^2}{2\sigma_1^2}}$, and thus the 3 dB line-width of the laser is $\Delta f = \frac{\sigma_1\sqrt{2\ln 2}}{\pi}$. The input rf signal of MZM is defined as $x(t) = m\cos(\omega_0 t + \phi)$, without loss of generality, setting ϕ=0; thus, the input rf signal of MZM is $x(t) = m\cos(\omega_0 t)$. The tunable FBG in this structure can be seen as a Gaussian filter so the spectral response is expressed as

$$B(\omega) = Be^{-\frac{[\omega-(\omega_c+\omega_0)]^2}{2\sigma_2^2}} \tag{3}$$

The 3 dB line-width of the laser is $BW = \frac{\sigma_2\sqrt{2\ln 2}}{\pi}$.

In summary, the electric field output from the MZM is obtained as

$$E_2(t) = \int_{-\infty}^{+\infty} F(w)e^{jwt}dw \cdot \cos(\varphi + m\cos(\omega_0 t)) \tag{4}$$

Whereas $M(t)$ is the second part of Eq. (4), that is [16],

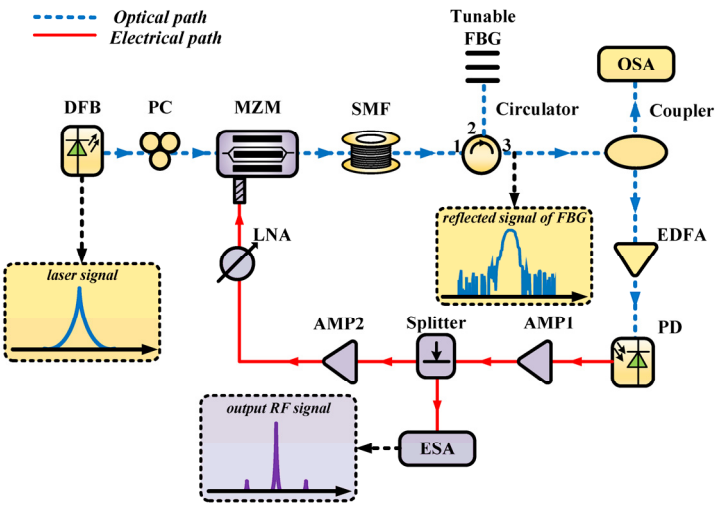

FIG. 1. Schematic diagram of the proposed OEO structure.

$$\begin{aligned} M(t) &= \cos(\varphi + m\cos(\omega_0 t)) \\ &= \cos(\varphi)\cos(m\cos(\omega_0 t)) - \sin(\varphi)\sin(m\cos(\omega_0 t)) \\ &= \cos(\varphi)J_0(m) - 2\sin(\varphi)J_1(m)\cos(\omega_0 t) \\ &+ 2\sum_{k=1}^{+\infty}(-1)^k \cos(\varphi)J_{2k}(m)\cos(2k\omega_0 t) \\ &+ 2\sum_{k=1}^{+\infty}(-1)^{k+1} \sin(\varphi)J_{2k+1}(m)\cos((2k+1)\omega_0 t) \end{aligned} \quad (5)$$

The Fourier transform of $M(t)$ is

$$\begin{aligned} M(\omega) &= 2\pi\cos(\varphi)J_0(m)\delta(\omega) - \sin(\varphi)J_1(m)[\delta(\omega-\omega_0)+\delta(\omega+\omega_0)] \\ &+ 2\sum_{k=1}^{+\infty}(-1)^k \cos(\varphi)J_{2k}(m)[\delta(\omega-2k\omega_0)+\delta(\omega+2k\omega_0)] \\ &+ 2\sum_{k=1}^{+\infty}(-1)^{k+1} \sin(\varphi)J_{2k+1}(m)[\delta(\omega-(2k+1)\omega_0)+\delta(\omega+(2k+1)\omega_0)] \end{aligned} \quad (6)$$

The Fourier transform of $E_2(t)$ is expressed as

$$E_2(\omega) = F(\omega) \otimes M(\omega) \quad (7)$$

where $\otimes$ is the symbol for convolution. Therefore, the frequency spectrum of the output signal from MZM is obtained as

$$\begin{aligned} E_2(\omega) &= 2\pi F(\omega) \otimes \{\cos(\varphi)J_0(m)\delta(\omega) - \sin(\varphi)J_1(m)[\delta(\omega-\omega_0)+\delta(\omega+\omega_0)] \\ &+ 2\sum_{k=1}^{+\infty}(-1)^k \cos(\varphi)J_{2k}(m)[\delta(\omega-2k\omega_0)+\delta(\omega+2k\omega_0)] \\ &+ 2\sum_{k=1}^{+\infty}(-1)^{k+1} \sin(\varphi)J_{2k+1}(m)[\delta(\omega-(2k+1)\omega_0)+\delta(\omega+(2k+1)\omega_0)]\} \end{aligned} \quad (8)$$

Using Eq. (8), we can easily compute the amplitude of each sideband signal.

As is evident from Table 1, the two largest signal amplitudes correspond to the carrier frequency and the first-order sideband; thus, the rf-signal output from the PD is

TABLE 1. The signal amplitude of every sideband and the corresponding filter gain

Order of sideband	Signal amplitude	Filter gain
2nd order	$-\cos(\varphi)J_2(m)$	$B(\omega_c+2\omega_0) = B\cdot e^{-\frac{\omega_0^2}{2\sigma_2^2}}$
1st order	$-\sin(\varphi)J_1(m)$	$B(\omega_c+\omega_0) = B$
Carrier frequency	$\cos(\varphi)J_0(m)$	$B(\omega_c) = B\cdot e^{-\frac{\omega_0^2}{2\sigma_2^2}}$
-1st order	$-\sin(\varphi)J_1(m)$	$B(\omega_c-\omega_0) = B\cdot e^{-\frac{4\omega_0^2}{2\sigma_2^2}}$
-2nd order	$-\cos(\varphi)J_2(m)$	$B(\omega_c-2\omega_0) = B\cdot e^{-\frac{9\omega_0^2}{2\sigma_2^2}}$

$$RF = K\sin(\varphi)J_1(m)\cos(\varphi)J_0(m)\cdot B^2 e^{-\frac{\omega_0^2}{2\sigma_2^2}}\cos(\omega_0 t) \quad (9)$$

where K is the gain of the PD [2], which implies that the gain of the OEO is

$$G_s = \frac{(G\cdot K\sin(\varphi)J_1(m)\cos(\varphi)J_0(m)B^2 e^{-\frac{\omega_0^2}{2\sigma_2^2}})^2}{m^2+A} \quad (10)$$

where G is the gain of the amplifier and A is the bias voltage [2]. With invariant bias and driving voltages, the expression $\sin(\varphi)J_1(m)\cos(\varphi)J_0(m)B^2 e^{-\frac{\omega_0^2}{2\sigma_2^2}}$ is obviously constant.

Setting $C = \sin(\varphi)J_1(m)\cos(\varphi)J_0(m)B^2 e^{-\frac{\omega_0^2}{2\sigma_2^2}}$ yields

$$G_s = \frac{(G\cdot K\cdot C)^2}{m^2+A} \quad (11)$$

If G $\frac{\sqrt{m^2+A}}{K\cdot C}$ is satisfied, then the OEO can be obtained by setting the signal gain of the loop.

III. EXPERIMENT

An experiment based on the setup illustrated in Fig. 1 was performed. The MZM (Fujitsu FTM7961EX) had a 3 dB bandwidth of 40 GHz and a half-wave voltage of 4.5 V. The PD (u^2t, XPDV2120R) had a 3 dB bandwidth of 50 GHz and a responsivity of 0.65 A/W. The rf amplifiers consisted of a low-noise amplifier (LNA) with a low noise amplitude of less than 4 dB, and a power amplifier (PA) with a gain of 17 dB. The DFB laser's optical power was approximately 13 dBm, and its bandwidth was 10 MHz. The erbium-doped fiber amplifier (EDFA) is a tunable optical amplifier, and was used to provide gain to the signal passed through optical devices and the 2 km SMF.

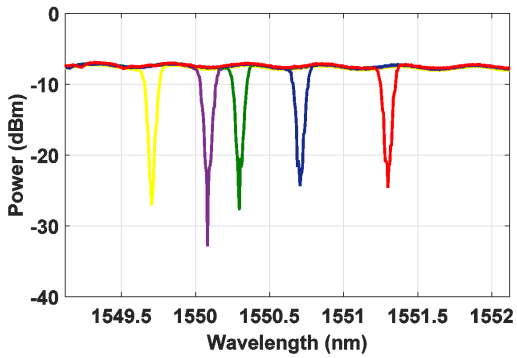

FIG. 3. Measured transmission frequency response of the tunable FBG used in the experiments.

The EDFA ensures that the PD can receive a sufficiently powerful optical signal to put out the rf signal.

The transmission and reflection response of the tunable FBG used in the experiments is shown in Fig. 3. We measured the transmission spectrum while changing the center frequency of the tunable FBG. Figure 3 shows the transmission spectrum of the tunable FBG. The tunable FBG was packaged in a box with a sponge block, for environmental stability. The central wavelength of the DFB laser was 1550.62 nm.

Figure 4 shows the spectrum of the optical signal, generated by the OEO. The reflected signal from the tunable FBG was modulated according to the laser signal: When the central frequency of the FBG was varied, the signal reflected from the tunable FBG was modulated to different positions beside the laser signal. Therefore, different rf signals were generated after the PD, which could beat different modulated light. Because of the limitations of our optical spectrum analyzer (OSA), the spectral peaks of the tunable FBG and laser were somewhat wide. The frequency span and resolution ratio settings were 0.8 and 0.005 nm, respectively.

Figure 5(a) shows the spectrum of the rf oscillation signal measured using an electrical spectrum analyzer (ESA) with a 1-MHz span and a 10-kHz resolution bandwidth. One strong oscillation signal appeared, accompanied by some low-level side modes. The Q value of the rf signal exhibited good performance; the side modes were suppressed effectively, with a suppression ratio was of 60 dB. Figure 5(b) shows the single-sideband phase noise spectrum of the generated tunable signal, which was used to evaluate the phase-noise performance. The measured results are shown in Fig. 5(b). The phase noise of the generated microwave signal was -117.2 dBc/Hz at an offset of 10 kHz. Notably, across the whole tunable range, the single-sideband phase noise was less than -102 dBc/Hz at the offset of 10 kHz. Figure 5(b) shows that the OEO system had a relatively low phase noise.

The frequency tunability of this OEO system was investigated. Tuning the central frequency of the FBG enabled the frequency of the rf oscillation signal to be tuned over a wide range. Figure 6 shows spectra of the generated signals when the frequency was tuned from 6 to 12 GHz, with a resolution bandwidth (RBW) of 3 MHz. The final rf-signal power in the oscillation was measured to be -7 dBm, and the deviation amplitude of the different oscillating signals was less than 2 dB. The harmonic signals measured in the electronic spectra were induced by the nonlinear amplification of the AMPs. The tuning range was further extended when a tunable FBG of wider

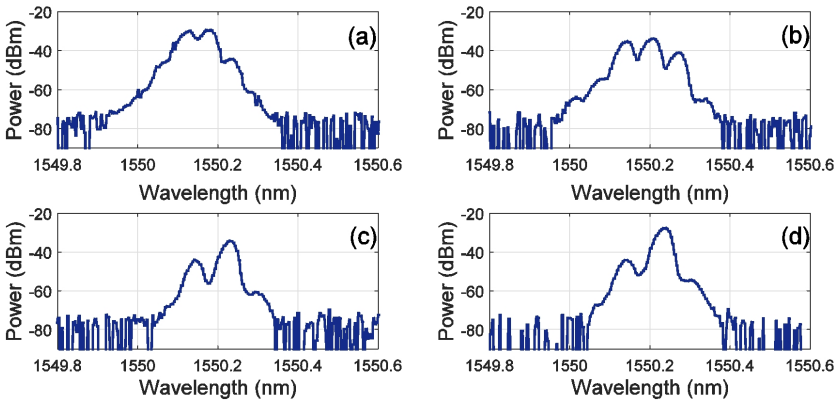

FIG. 4. Spectra of the optical signals generated by the OEO, for different central frequencies of the FBG.

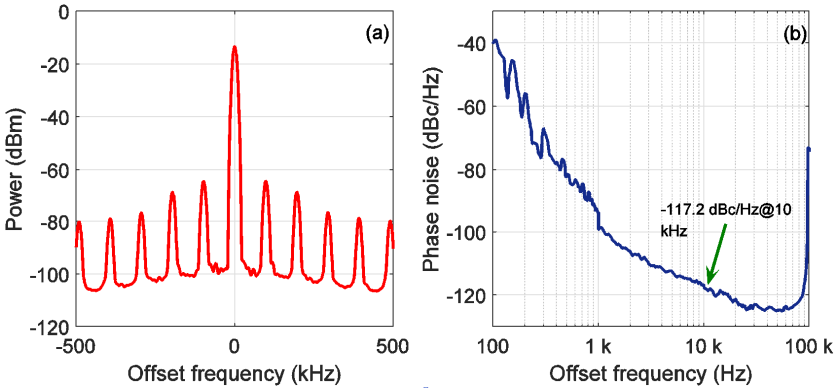

FIG. 5. Measured spectrum of (a) the rf oscillation signal and (b) the phase noise of the generated 10.2-GHz microwave signal.

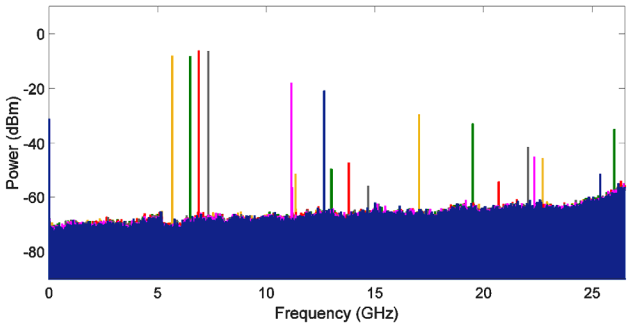

FIG. 6. Spectra of the generated signal when the frequency was tuned from 6 to 12 GHz.

reflection bandwidth was used, and the bandwidth of the rf amplifier was increased. In the traditional structure, the laser bandwidth dramatically affects the rf quality. A wide-spectrum laser reduced the purity of the rf signal, and the proposed device generated a wide-spectrum rf signal after the PD.

IV. CONCLUSION

In this paper, we demonstrated a low-cost and simple wideband-tunable OEO. A tunable range from 6 to 12 GHz was realized using this configuration. The measured single-sideband phase noise was -117.2 dBc/Hz at 10 kHz of the generated GHz signal. A tunable OEO structure with the aforementioned demonstrated advantages will be useful for realizing many inexpensive, small optical systems, including FBG sensors and radar identification system.

ACKNOWLEDGMENT

This work was supported by the China Postdoctoral Science Foundation (2016T90995), and the National Natural Science Foundation of Jiangsu Province (BK20150715).

REFERENCES

1. X. S. Yao and L. Maleki, "Optoelectronic oscillator for photonic systems," IEEE J. Quantum Electron. **32**(7), 1141-1149 (1996).
2. X. S. Yao and L. Maleki, "High frequency optical subcarrier generator," Electron, Lett. **30**(18), 1525-1526 (1994).
3. Y. Teng, Y. Chen, B. Zhang, J. Li, L. Lu, and P. Zhang, "Tunable single-mode injection-locked optoelectronic oscillator with low phase-noise," Optik **127**(10), 4312-4314 (2016).
4. W. Li and J. Yao, "Optically tunable frequency-multiplying optoelectronic oscillator," IEEE Photon. Technol. Lett. **24**(10), 812-814 (2012).
5. W Li and J. Yao, "A wideband frequency tunable optoelectronic oscillator incorporating a tunable microwave photonic filter based on phase-modulation to intensity-modulation conversion using a phase-shifted fiber Bragg grating," IEEE Trans. Microw. Theory Techn. **60**(6), 1735-1742 (2012).
6. D. Zhu, S. Pan, and D. Ben, "Tunable frequency-quadrupling dual-loop optoelectronic oscillator," IEEE Photon. Technol. Lett. **24**(3), 194-196 (2012).
7. S. Chin and L. Thévenaz, "Recent advancement of slow light in microwave photonics applications," in *IEEE International Topical Meeting on Microwave Photonics* (2010), pp. 385-388.
8. X. Xie, C. Zhang, T. Sun, P. Guo, X. Zhu, L. Zhu, W. Hu, and Z. Chen, "Wideband tunable optoelectronic oscillator based on a phase modulator and a tunable optical filter," Opt. Lett. **38**(5), 655-662 (2013).
9. W. Chen, A. Wen, Y. Gao, N. Yao, Y. Wang, M. Chen, and S. Xiang, "Photonic generation of binary and quaternary phase-coded microwave waveforms with frequency quadrupling," IEEE Photon. J. **8**(2), 1-8 (2016).
10. B. Yang, X. Jin, X. Zhang, S. Zheng, H. Chi, and Y. Wang, "A wideband frequency-tunable optoelectronic oscillator based on a narrowband phase-shifted FBG and wavelength tuning of laser," IEEE Photon. Technol. Lett. **24**(1), 73-75 (2012).
11. B. Lin, M. Jiang, S. C. Tjin, P. P. Shum, Y. Ge, and Y. He, "Tunable microwave generation based on a phase-shifted chirped fiber Bragg grating," in *Eighth International Conference on Wireless and Optical Communications Networks IEEE* (2011), pp. 1-3.
12. N. Q. Ngo, S. Y. Li, L. N. Binh, and S. C. Tjin, "A phase-shifted linearly chirped fiber Bragg grating with tunable bandwidth," Opt. Commun. **260**(2), 438-441 (2006).
13. B. Lin and S. C. Tjin, "Advanced fiber Bragg grating for tunable microwave generation," in *International Conference on Optical Communications and Networks IEEE* (2017).
14. B. Lin, S. C. Tjin, M. Jiang, and P. Shum, "Tunable microwave generation based on a dual-wavelength fiber laser with an inverse-Gaussian apodized fiber Bragg grating," Appl. Opt. **50**(25), 4912-4916 (2011).
15. K. O. Hill and G. Meltz, "Fiber Bragg grating technology fundamentals and overview," J. Lightw. Technol. **15**(8), 1263-1276 (1997).
16. Y. Teng, Y. Chen, B. Zhang, J. Li, L. Lu, Y. Zhu, and P. Zhang, "Generation of low phase-noise frequency-sextupled signals based on multimode optoelectronic oscillator and cascaded Mach-Zehnder modulators," IEEE Photon. J. **8**(4), 1-8 (2017).